Singularities and avalanches in interface growth with quenched disorder

Hernán A. Makse
Center for Polymer Studies and Department of Physics, Boston University, Boston, Massachussetts 02215
(Received 4 April 1995)

A simple model for an interface moving in a disordered medium is presented. The model exhibits a transition between the two universality classes of interface growth in the presence of quenched disorder. Using this model, it is shown that the application of constraints to the local slopes of the interface produces avalanches of growth that become relevant in the vicinity of the depinning transition. The study of these avalanches reveals a singular behavior at the depinning transition that explains a recently observed divergency in the equation of motion of the interface. The anisotropy in the medium is also studied as a possible source of the divergency in the equation of motion.

PACS number(s): 47.55.Mh, 68.35.Fx

The problem of interface motion in disordered media has attracted considerable attention recently [1]. In a typical realization of the problem a d-dimensional interface moves in a $(d+1)$-dimensional disordered medium, driven by an external force F. The interface is assumed to be oriented along the longitudinal $\vec{x}$ direction, and is specified by the height $y(\vec{x},t)$. For small forces the interface is pinned by the random quenched impurities of the medium, and the average velocity is zero. Above a critical value F_c, the external force overcomes the effect of the impurities, and the interface moves with a finite velocity. Near the threshold, the velocity scales as

$$v \sim f^{\theta}, \tag{1}$$

where $f \equiv F/F_c - 1$ is the reduced force, and θ the velocity exponent.

The fluctuations of the interface are characterized by the scaling of the local interface width $w(\ell)$ with the size of the window of observation ℓ

$$w(\ell) \sim \ell^{\alpha}. \tag{2}$$

The roughness exponent α characterizes the different universality classes of interface growth phenomena.

In a recent numerical study, Amaral *et al.* [2] have shown that the universality classes can also be classified according to the behavior of the coefficient λ of a nonlinear term of the form $(\nabla y)^2$ in the equation of motion of the interface.

One of the universality classes is described by an equation similar to the Kardar-Parisi-Zhang (KPZ) equation [3] but with a quenched disorder term $\eta(\vec{x},y)$

$$\partial_t y(\vec{x},t) = \nabla^2 y + \lambda(\nabla y)^2 + \eta(\vec{x},y) + F \tag{3}$$

with the coefficient λ diverging at the depinning transition as

$$\lambda(f) \sim f^{-\phi}, \tag{4}$$

where $\phi \simeq 0.64$ [2]. The roughness exponent at the depinning transition in $(1+1)$ dimensions is $\alpha \simeq 0.63$ and can be obtained by a mapping onto directed percolation [4,5]. We refer to this universality class as directed percolation depinning (DPD).

A second universality class is described, at the depinning transition, by an equation of the Edwards-Wilkinson type [6] with quenched disorder

$$\partial_t y(\vec{x},t) = \nabla^2 y + \eta(\vec{x},y) + F. \tag{5}$$

Models with $\lambda = 0$ (for any force), or $\lambda \to 0$ (when $F \to F_c^+$), belong to the universality class of (5). Analytical [7] and numerical [8] (using the height-height correlation function) studies in $(1+1)$ dimensions yield a roughness exponent $\alpha \simeq 1$. However, an anomalous exponent $\alpha \simeq 1.23 - 1.25$ [9–11] is found when the scaling of the total interface width, $W(L) \sim L^{\alpha}$, with the system size L is used to calculate the roughness exponent. This universality class is referred to as quenched Edwards-Wilkinson (QEW).

In this paper we study the possible mechanisms that generate the different scaling behavior inherent to each universality class. In particular, we study the origin of the singularity in the coefficient λ observed for the DPD universality class.

In the first part of the paper, we argue that the different universality classes arise due to constraints imposed on the local slopes of the interface. To illustrate this point, we introduce a simple model that exhibits a transition between the two universality classes of interface growth in disordered media. When the constraint to the slopes is absent, the QEW universality class is obtained, and a super-rough interface [12], characterized by a roughness exponent $\alpha \geq 1$, is found. On the other hand, the DPD result is obtained when longitudinal— along the $\vec{x}$ direction— fluctuations of the interface height are allowed, *and* the growth rule is restricted by a generalized solid-on-solid (SOS) condition.

The generalized SOS condition is a universal feature appearing in all the models of the DPD universality class. It is referred to as "erosion of overhangs" in Ref. [5], and it is analogous to the restricted SOS condition that imposes a bound in the local slope of the interface $|y(x \pm 1,t) - y(x,t)| \leq 1$. The restricted SOS condition was originally introduced in simple models of growth with *time-dependent* noise [13]. In these type of models, the constraint to the slopes is commonly associated with lon-

gitudinal propagation of growth that generates nonlinearities in the equation of motion. Moreover, we show that in the presence of *quenched* disorder, these constraints also generate *avalanches of growth.* These avalanches are irreversible growth events that become relevant near the depinning transition. We show that the avalanches display a singular behavior at the depinning transition that is responsible for the divergence in the coefficient λ.

In the second part of the paper, we discuss our results in light of a recent study by Tang *et al.* [14]. In particular, the anisotropy in the medium is studied as a possible source of the nonlinearity $\lambda(\nabla y)^2$ at the depinning transition.

Consider a one-dimensional elastic interface moving in a two-dimensional disordered medium of longitudinal size L. A discrete model for such an interface is defined in the square lattice by the height values $\{y_k\}_{k=1,\ldots,L}$. The interface moves under the influence of an external force $\vec{F} = (0, F)$, and fluctuates in the *longitudinal* or x direction, and *transversal* or y direction. The strength of these fluctuations is controlled by the elastic constants ν_x and ν_y, respectively. For the kth column and at a given time, the x and y components of the total force vector are given by

$$f_y(k) = \nu_y\,(y_{k+1} + y_{k-1} - 2y_k) + \eta(k, y_k) + F, \quad \text{(6a)}$$

$$f_x(k) = -\nu_x + \eta(k, y_k). \quad \text{(6b)}$$

The first term on the right hand side of (6a) includes the elastic force acting to make the interface smooth. For the x direction we include a constant force of value $-\nu_x$ that mimics the elastic nearest-neighbor interaction, and opposes longitudinal motions [15]. The random force, which mimics the effect of quenched disorder in the medium, is represented by $\eta(k, y_k)$, and it is an uncorrelated random number with uniform probability distribution between $[-\Delta, \Delta]$. η represents a repulsive force for positive values and an attractive or pinning force for negative values. A site at the interface moves forward or laterally only when the respective total force becomes bigger than zero. Therefore, the kth column and its nearest neighbors are updated in the following way:

$$y_k = y_k + 1 \quad \text{if} \quad f_y(k) > 0, \quad \text{(7a)}$$

$$y_{k+1} = y_k \quad \text{if} \quad f_y(k) > 0, \quad \text{(7b)}$$

$$y_{k-1} = y_k \quad \text{if} \quad f_x(k) > 0.$$

Equations (6a) and (7a) correspond to the model introduced by Leschhorn [9] to study an elastic interface described by the QEW equation, and they are equivalent to the discretization of (5). Equations (6b) and (7b) are the simplest generalization of the model to include longitudinal motions. A longitudinal motion to a nearest-neighbor column is allowed if the neighboring column is smaller than the column considered. After the longitudinal motion, the interface becomes a multivalued function of the longitudinal coordinate x [see Fig. 1(a)]. The generalized

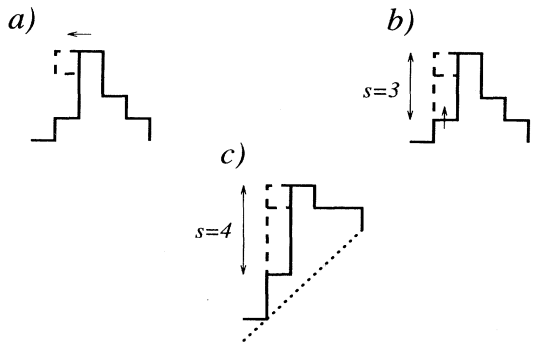

FIG. 1. Sketch of the effect of longitudinal motions of a site at the interface: (a),(b) for an untilted interface, and (c) for a tilted interface with $m = 1$ as defined in the text. A longitudinal motion (a) produces an effective avalanche (b) in the nearest-neighbor column due to the application of the generalized SOS condition. The size of the avalanche, s, is larger for the tilted interface than for the untilted one, as can be seen comparing (b) and (c).

SOS condition is then applied in order to transform the interface into a single-valued function, by defining the interface with the highest value of the height. This process generates a *transversal avalanche of growth* in the neighboring column, as shown in Fig. 1(b). This growth event occurs regardless of the value of the noise in the neighboring column.

We perform numerical simulations in a square lattice of size $L = 1024$. Helical boundary conditions $y_L = y_1 + m\,L$, where $m \equiv \langle \nabla y \rangle$ is the average external tilt, are imposed on the interface in order to study the interface velocity as a function of the tilt [16,17]. Figure

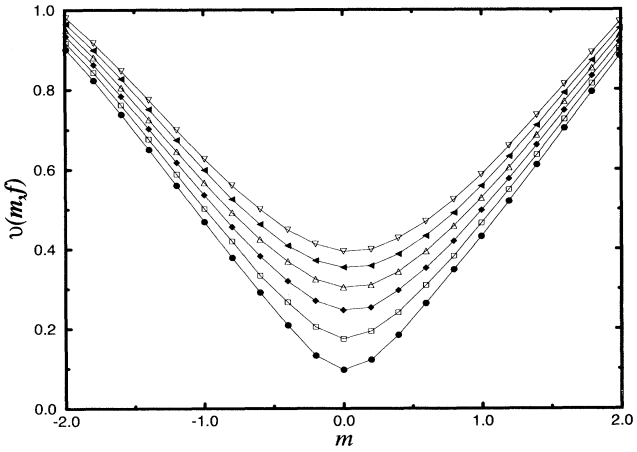

FIG. 2. Plot of the velocity $v(m, f)$ as a function of the average tilt m of the interface for values of the reduced force from $f = 0.19$ (bottom) to $f = 1.38$ (top). The parameters are $\nu_x = 0.4$, $\nu_y = 1.0$, and $\Delta = 3.0$. The system size is $L = 1024$, and results are averaged over 50 independent realizations of the disorder. The "closing" of the parabolas shows that a diverging nonlinear coefficient is present in the equation of motion, as was observed in Ref. [2].

2 shows the tilt dependence of the velocity of the interface for the value $\nu_x = 0.4$. In the following, we fix the values $\nu_y = 1.0$ and $\Delta = 3.0$, since our results do not depend on these parameters. We see a parabolic dependence of the velocity with the tilt, with the parabolas becoming steeper when $F \to F_c^+$ corresponding to an increase in λ as in (4). This fact indicates that the model belongs to the DPD universality class for this choice of ν_x. Moreover, the model presents a transition at a critical value ν_{x_c}. If the value of ν_x is increased such that $\nu_x \geq \nu_{x_c} = \Delta$, then the QEW result is found. Specifically, we find that v is independent of m, indicating that $\lambda = 0$ for any force. The fact that f_x is always negative for $\nu_x > \Delta$ explains this transition: longitudinal motions cannot occur and one recovers the model of Ref. [9].

The different parabolas obtained for a given value of $\nu_x < \nu_{x_c}$ can be rescaled using the scaling ansatz [2]

$$v(m, f) \sim f^{\theta}\, g(m^2/f^{\theta+\phi}), \tag{8}$$

where g is a universal scaling function. Support for (8) is provided by the data collapse shown in Fig. 3, where we replot the data of Fig. 2 and the data obtained for $\nu_x = 1.2$, $\nu_x = 2.0$, and $\nu_x = 2.8$ [18]. The scaling function g becomes flatter as $\nu_x \to \nu_{x_c}^-$, indicating that the prefactor of λ in (4) goes to zero, even though the singularity associated with f is still present as long as $\nu_x < \nu_{x_c}$.

In the following, we argue that the divergence in λ is explained by the singular behavior of the size of the avalanches of growth produced by the generalized SOS condition.

According to (7), the interface can advance in two independent ways. One way is via a transversal motion (if $f_y > 0$), and the other is via a longitudinal motion (if $f_x > 0$) plus the transversal avalanche in the neighboring column. In order to determine the relevant growth mechanism near the depinning transition, we study the mean value of the number of longitudinal and transversal motions per unit time n_x and n_y, respectively, as a function of the force. For a DPD interface characterized by $\nu_x = 0.4$, we find

$$n_x(f) \sim f^{\gamma_x}, \qquad n_y(f) \sim f^{\gamma_y}, \tag{9}$$

with $\gamma_x \simeq 0.60$ and $\gamma_y \simeq 0.78$. Both quantities go to zero at F_c, since the velocity vanishes at the depinning transition. However, the ratio $n_x/n_y \sim f^{-0.18}$ diverges at F_c, indicating the *relevance* of longitudinal fluctuations for the motion of the interface at the depinning transition. This fact might be explained as follows. For forces close to F_c the velocity is almost zero and the interface moves in a very irregular way, jumping from one metastable pinning configuration to another. In this "jerky" motion the interface takes advantage of longitudinal motions, rather than transversal ones, to surround and overcome the impurities, and the ratio n_x/n_y increases near F_c. This also implies that *avalanche events become relevant for the motion of the interface only in the vicinity of the depinning transition.*

We also study the mean value of the size of the avalanches produced by the generalized SOS condition per unit time $\langle s \rangle$ as a function of the tilt and for different forces. Figure 4 shows the results. As it turns out, $\langle s \rangle$, as well as the velocity [26], has a parabolic dependence on m. These parabolas become steeper as $F \to F_c^+$, and we can fit $\langle s \rangle$ to

$$\langle s \rangle = s_0 + \lambda_s\, m^2, \tag{10a}$$

with

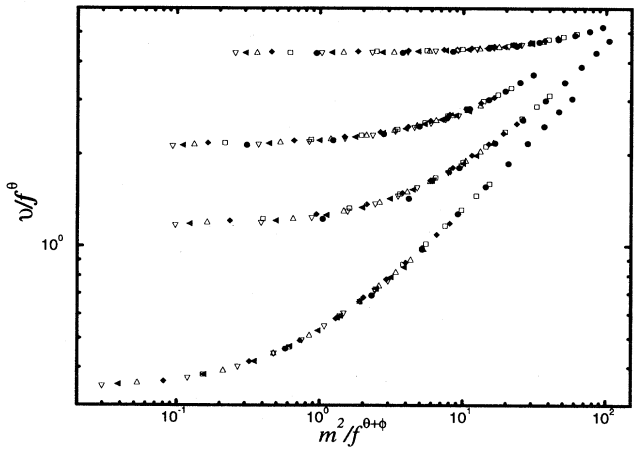

FIG. 3. Data collapse of the data of Fig. 2 ($\nu_x = 0.4$) and the data corresponding to $\nu_x = 1.2$, $\nu_x = 2.0$, and $\nu_x = 2.8$ (shown from bottom to top, respectively), plotted according to the scaling relation of Eq. (8). The scaling function becomes flatter as $\nu_x \to \nu_{x_c}^- = \Delta$, indicating the transition to the QEW universality class. Each set of curves is shifted for clarity.

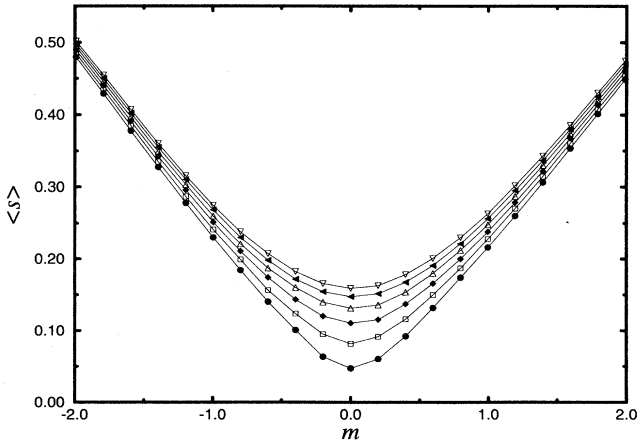

FIG. 4. Plot of the average size of the avalanches $\langle s \rangle$ produced by the generalized SOS condition as a function of the tilt m, for the same forces and parameters as in Fig. 2.

$$\lambda_s \sim f^{-\phi} \tag{10b}$$

and $\phi \simeq 0.64$ the same exponent as in (4). The parabolas can also be rescaled using the scaling ansatz (8) with the same value of θ used for the velocity curves.

As shown in Fig. 1(c), the size of an avalanche is larger for the tilted interface than for the untilted one. This explains the increase of $\langle s \rangle$ with the tilt, exemplified in Fig. 4 for a given fixed force. Moreover, since the relative occurrence of longitudinal motions and avalanches is larger near the depinning transition than away from it [see Eq. (9)], the same external tilt will cause a larger increase in the average $\langle s \rangle$ near F_c than for $F \gg F_c$. Thus the coefficient λ_s that measures the variation experienced by $\langle s \rangle$ due to a change in the average tilt of the interface, increases its value as $F \to F_c^+$ and the parabolas become steeper.

Notice that the relevance of longitudinal motions and avalanches of growth near F_c implies that the velocity is determined by the size of the avalanches, $v \propto \langle s \rangle$, so that $\lambda \propto \lambda_s$. Thus, we argue that the singularity of the coefficient λ can be explained by the same divergence observed in λ_s. The motion of the interface near the depinning transition is entirely dominated by the avalanches of growth produced by the generalized SOS condition.

The same behavior can be predicted for the other models of the DPD universality class. All these models share a constraint in the growth rule of the interface height that generates avalanches analogous to the ones in the present model. In the model of Ref. [4] a slope constraint is applied to the interface that implies a readjustment of the height regardless of the value of the noise. The so-called erosion of overhangs in the model of Ref. [5] corresponds to our generalized SOS condition. And the model of Ref. [19] presents a restricted SOS condition that produces avalanches of growth (see Ref. [20]).

The relevance of the constraint imposed on the slopes might explain some experimental results as well. The agreement between the exponents of the paper burning experiment of Ref. [24] and the imbibition experiments of Ref. [5], with the exponents of the DPD universality class, can be understood due to the erosion of the invaded region observed in experiments being analogous to the erosion of overhangs imposed in the numerical models.

Next, we discuss our results in light of a recent analytical study by Tang *et al.* [14]. In this study the universality classes are classified according to the dependence of the threshold force on the slope $F_c(m)$, instead of the dependence of the velocity $v(m, f)$ on the slope, as was originally proposed by Amaral *et al.* [2]. Tang *et al.* also propose a set of scaling relations that explain most of the exponents obtained in the numerical calculations [2]. They also show that for the DPD class of models the critical force depends on the external tilt in the form [14]

$$F_c(m) - F_c(m=0) \sim -|m|^{1/\nu(1-\alpha)}, \tag{11}$$

where ν is the correlation length exponent, so that the interface tilted away from the horizontal direction ($m = 0$) is characterized by a smaller depinning threshold. In terms of our results, the slope dependence of the threshold can be related to the presence of the SOS condition, since a tilted interface favors the occurrence of avalanches that, in turn, results in a decrease of the critical force needed for the motion of the interface.

A more general question points to what are the mechanisms that induce such slope dependence in the depinning threshold. In this regard, Tang *et al.* argue that an anisotropic random force, characteristic for an anisotropic disordered medium, is a possible mechanism that generates such slope dependence. They propose the flux line in superconductors as a typical example where the proposed mechanism is present. The motion of the flux line is the result of three different forces [14,21]: (i) a smoothing line tension term; (ii) a Lorentz force perpendicular to the line; and (iii) the anisotropic random force due to disorder in the medium.

To study the effects of the anisotropy of the medium, we introduce a model for the anisotropic flux line that incorporates the above considerations. We consider the line to be described by an internal coordinate σ ($0 \leq \sigma \leq 1$) that parametrizes the position of the flux line $\vec{r}(\sigma) \equiv (x(\sigma), y(\sigma))$ confined in a two-dimensional plane.

The three terms contributing to the local velocity of the flux line $d\vec{r}/dt$ are the following:

(i) A line tension term given by $-(1/\sqrt{g})\delta A/\delta \vec{r}$ that minimizes the line energy $A = \int_0^1 \sqrt{g}\, d\sigma$, where $g = |d\vec{r}/d\sigma|^2$.

(ii) A Lorentz force $\vec{F} = F\hat{n}$, where $\hat{\vec{n}}(\sigma) = (n_x, n_y)$ is the unit normal at position $\vec{r}(\sigma)$, and $F = |\vec{F}|$ is constant.

(iii) An anisotropic random force $\vec{\eta}(\sigma) = (\eta_x(\sigma), \eta_y(\sigma))$ that describes the effects of the impurities, where η_x and η_y are uncorrelated random forces with zero mean and amplitudes Δ_x and Δ_y, respectively. The anisotropic case corresponds to $\Delta_x \neq \Delta_y$.

We propose the following equation of motion for the anisotropic flux line:

$$\frac{d\vec{r}(\sigma)}{dt} = -\frac{1}{\sqrt{g}}\frac{\delta A}{\delta \vec{r}(\sigma)} + F\hat{\vec{n}}(\sigma) + \vec{\eta}(\sigma). \tag{12}$$

A similar equation was considered by Maritan *et al.* [22] to study the dynamical behavior of a growing interface in time-dependent noise dominated problems. Notice that this formulation allows for overhangs and it is invariant under a general reparametrization of the curve [22,23].

A numerical integration of such an equation is quite complicated, so we now introduce a model that corresponds to the discrete version of (12), and is in the spirit of the model of Eqs. (6) and (7). The proposed flux line model can be thought as a set of L beads. We identify the internal coordinate σ with the label k of each bead. Then $\vec{r}_k = (x_k, y_k)$, $(k = 1, \ldots, L)$ specifies the position of the kth bead on the two-dimensional lattice. We consider only integer values of x_k and y_k, and we impose periodic boundary conditions. For each bead we calculate a vector force $\vec{f}(k) = (f_x(k), f_y(k))$ according to

$$f_x(k) = -\frac{1}{\sqrt{g_k}}\frac{\delta A}{\delta x_k} + F n_x(k), \tag{13a}$$

$$f_y(k) = -\frac{1}{\sqrt{g_k}}\frac{\delta A}{\delta y_k} + F n_y(k), \tag{13b}$$

where $g_k = (x_{k+1} - x_k)^2 + (y_{k+1} - y_k)^2$, and $A = \sum_{k=1}^{L}\sqrt{g_k}$ is the discretization of the line energy of the flux line. The strength of the external force $F = |\vec{F}|$ is kept constant, and its direction is determined by the local unit normal at each position k, $\hat{\vec{n}} = (n_x(k), n_y(k))$. A regularization condition is applied so that the beads are not allowed to occupy the same column at the same time. A random force $\vec{\eta} = (\eta_x(k), \eta_y(k))$ is defined for

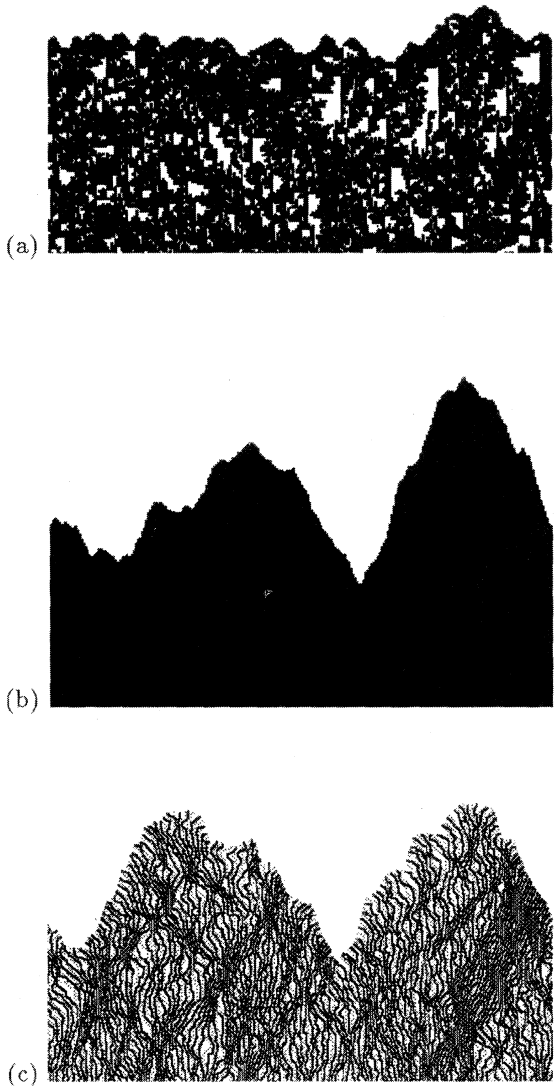

FIG. 5. Three different interfaces at the depinning transition of the models considered in this paper. (a) A typical DPD interface at the depinning transition. The holes left behind by the interface correspond to the application of the generalized SOS condition after a longitudinal motion of a site at the interface occurs. The holes are situated in regions of strong disorder strength, so that the interface overcomes these pinning regions by longitudinal motions plus the application of the generalized SOS condition [see Fig. 1(b)]. (b) A typical QEW interface at the depinning transition. Since no longitudinal motions occur, the holes have disappeared. Notice the large slopes developed due to the absence of constraints to the local slopes of the interface. (c) A typical anisotropic flux line "interface" characterized by anisotropic random forces of strength $\Delta_x = 2.0$ and $\Delta_y = 3.0$. The trajectories of the even beads are plotted in black, and the trajectories of the odd beads are plotted in gray. The flux line takes advantage of the allowed longitudinal motions to surround the strong pinning configurations, as can be observed in the trajectories of the beads. Also, since $\Delta_x < \Delta_y$, longitudinal motions are more favorable than transversal motions. However, the fact that the flux line develops large slopes at the depinning transition, as the QEW interface, suggests that all these mechanisms become "irrelevant" at the critical point. The absence of constraints in the local slopes generates an interface characterized by large slopes and a roughness exponent close to one, as is observed also for the QEW interface.

every point in the lattice. η_x and η_y are uncorrelated random numbers uniformly distributed between $[0, \Delta_x]$ and $[0, \Delta_y]$, respectively. We start with a flat configuration at time $t = 0$, and for a given time t the position of the kth bead is updated when the total force overcomes the pinning effect of the impurities,

$$\begin{aligned} y_k &= y_k + 1 \quad \text{if} \quad f_y(k) > \eta_y(k), \\ y_k &= y_k - 1 \quad \text{if} \quad f_y(k) < -\eta_y(k), \end{aligned} \tag{14a}$$

$$\begin{aligned} x_k &= x_k + 1 \quad \text{if} \quad f_x(k) > \eta_x(k), \\ x_k &= x_k - 1 \quad \text{if} \quad f_x(k) < -\eta_x(k). \end{aligned} \tag{14b}$$

We have simulated this anisotropic flux line model for two different sets of the strengths of the anisotropic random forces: $\Delta_x = 2$, $\Delta_y = 3$ and $\Delta_x = 3$, $\Delta_y = 2$. Figure 5(c) shows a typical "interface" at the depinning transition obtained with the proposed flux line model, together with an interface corresponding to the DPD model [Fig. 5(a)] defined by (6) and (7) for $\nu_x = 0.4$, and a QEW interface (5b) defined by (6) and (7) for $\nu_x = 3.0$. Notice the similarity between the QEW interface and the flux line model: both models develop large slopes at the depinning transition. This similitude is due to the fact that both models are free of constraints in the local slopes. A rather different interface is obtained when constraints to the growth of the local slopes are imposed, as can be observed for the DPD interface.

In our numerical simulation with the flux line model, we first focus on the slope dependence of the threshold force. We start from a flat line at time $t = 0$, and we apply a small external force F. Growth proceeds according to Eqs. (13) and (14) until the flux line reaches the first pinning configuration and stops. Then, the value of the force is slightly increased so that the line will move until the next pinning configuration. The threshold force F_c, corresponding to a given system size, is identified as the force for which the flux line moves a distance of the order of the system size without finding a pinning configuration. Figure 6(a) shows the threshold force $F_c(m)$ as a function of the tilt m for the anisotropic flux line. Contrary to the behavior of the DPD models for which a decrease of the critical force with the tilt is expected [see Eq. (11)], we find that for the anisotropic flux line the critical force increases with the tilt for both sets of disorder strengths. We have also studied the slope dependence of the velocity $v(m, f)$ in order to identify the effective coefficient $\lambda(f)$. We were able to identify a negative coefficient λ that goes to zero at the depinning transition. However, due to the large fluctuations of the velocity near the depinning transition, our numerical results are not good enough to obtain an estimation of the exponent ϕ. We notice that a negative vanishing λ is consistent with our findings for the threshold force. We also study the scaling of the local width w with the size ℓ of the window of observation $w(\ell) \sim \ell^{\alpha}$, and we find a roughness exponent $\alpha \simeq 0.83$ at the depinning transition [Fig. 6(b)]. We are left with the conclusion that the anisotropic flux line model considered in this study does not belong to the DPD universality class. However, we notice that the value of the roughness exponent is smaller than the expected value for the QEW universality, for which $\alpha \simeq 1$ is found [25]. Therefore, we cannot conclude that the flux line model belongs to this universality class either.

We wish to point out that the fact that we did not find a DPD behavior in the proposed anisotropic flux line model does not rule out the possibility that other forms of anisotropy might generate a diverging λ term at the depinning transition, or the slope dependence in the threshold force argued in [14]. A potentially important difference between the discrete flux line model studied here and the continuum model considered by Tang *et al.* is that in Ref. [14] only the normal motion to the interface plays a role, while the discrete flux line has an internal structure, and we have explicitly included longitudinal motions. A more general study is needed, and we propose that other models of interface growth in disordered media

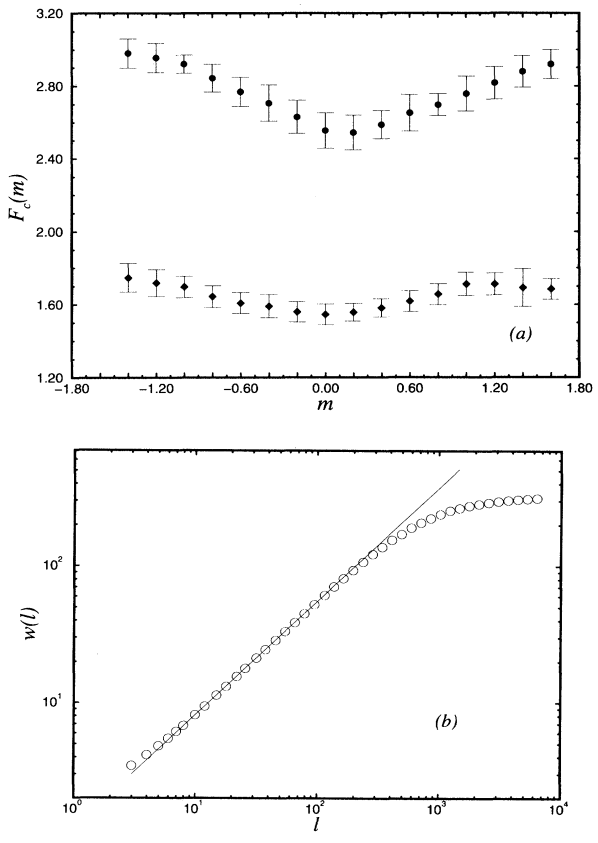

FIG. 6. (a) Threshold force $F_c(m)$ for the anisotropic flux line model as a function of the external slope m for disorder strengths $\Delta_x = 2$, $\Delta_y = 3$ (top), and $\Delta_x = 3$, $\Delta_y = 2$ (bottom). (b) Log-log plot of the local width $w(\ell)$ at the depinning transition for the flux line model as a function of the size of the window of observation ℓ for disorder strengths $\Delta_x = 2$ and $\Delta_y = 3$. The system size is $L = 8196$ and we average over 100 realizations of the disorder. The dashed line corresponds to a least squares fit and has slope $\alpha \simeq 0.83$.

which might be suitable to include anisotropic effects, such as the random field or random bond Ising model [26], or the fluid invasion model [27], should be considered as well.

In conclusion, we present a simple model for an elastic interface moving in a disordered medium, which captures the relevant features of the two universality classes. The origin of the singular behavior in the equation of motion of the DPD class of models is explained by simple microscopic constraints— such as the erosion of overhangs in Ref. [5] or restricted SOS in [4]— imposed on the local slopes of the interface that generates irreversible avalanches of growth. Our results are discussed in light of a recent study by Tang *et al.*, where it was proposed that the anisotropy in the medium generates a DPD behavior. We introduce and study a reparametrization invariant flux line model for which the anisotropy can naturally be considered. We find that the model does not present the expected DPD behavior. However, we argue that other manifestations of the anisotropy should be considered as well, and more numerical work needs to be done in order to determine the effects of the anisotropy on the motion of interfaces in disordered media.

I wish to thank S. Tomassone, L. Amaral, R. Cuerno, S. Harrington, P. Ch. Ivanov, D. Langtry, K. Lauritsen, H. Leschhorn, P. Rey, R. Sadr-Lahijany, and H. E. Stanley for useful suggestions and discussions. The Center for Polymer Studies is supported by the National Science Foundation.

[1] *Dynamics of Fractal Surfaces*, edited by F. Family and T. Vicsek (World Scientific, Singapore, 1991); T. Halpin-Healey and Y.-C. Zhang, Phys. Rep. **254**, 215 (1995); A.-L. Barabási and H. E. Stanley, *Fractal Concepts in Surface Growth* (Cambridge University Press, Cambridge, 1995).

[2] L. A. N. Amaral, A.-L. Barabási, and H. E. Stanley, Phys. Rev. Lett. **73**, 62 (1994); L. A. N. Amaral, A.-L. Barabási, H. A. Makse, and H. E. Stanley, Phys. Rev. E (to be published).

[3] M. Kardar, G. Parisi, and Y.-C. Zhang, Phys. Rev. Lett. **56**, 889 (1986).

[4] L.-H. Tang and H. Leschhorn, Phys. Rev. A **45**, R8309 (1992).

[5] S. V. Buldyrev, A.-L. Barabási, F. Caserta, S. Havlin, H. E. Stanley, and T. Vicsek, Phys. Rev. A **45**, R8313 (1992).

[6] S. F. Edwards and D. R. Wilkinson, Proc. R. Soc. London Ser. A **381**, 17 (1982).

[7] T. Nattermann, S. Stepanov, L.-H. Tang, and H. Leschhorn, J. Phys. (France) II **2**, 1483 (1992); O. Narayan and D. S. Fisher, Phys. Rev. B **48**, 7030 (1993).

[8] M. Dong, M. C. Marchetti, A. A. Middleton, and V. Vinokur, Phys. Rev. Lett. **70**, 662 (1993).

[9] H. Leschhorn, Physica A **195**, 324 (1993).

[10] H. Leschhorn and L.-H. Tang, Phys. Rev. Lett. **70**, 2973 (1993)

[11] H. A. Makse and L. A. N. Amaral, Europhys. Lett. (to be published).

[12] S. Das Sarma, S. V. Ghaisas, and J. M. Kim, Phys. Rev. E **49**, 122 (1994).

[13] J. M. Kim and J. M. Kosterlitz, Phys. Rev. Lett. **62**, 2289 (1989).

[14] L.-H. Tang, M. Kardar, and D. Dhar, Phys. Rev. Lett. **74**, 920 (1995).

[15] A term analogous to the elastic force acting in the y direction cannot be considered for the x direction because the model does not allow for overhangs.

[16] According to (3), for a tilted interface with tilt m, the average velocity becomes $v(m) = v_0 + \lambda\, m^2$, where v_0 is the velocity of the untilted interface [2,17]. Thus one can gain information on the presence and magnitude of the nonlinear coefficient λ by monitoring the velocity of the interface as a function of the average tilt, and fitting to a parabola the obtained curve.

[17] J. Krug and H. Spohn, Phys. Rev. Lett. **64**, 2332 (1990).

[18] We use $\phi \simeq 0.64$ for all values of ν_x in the data collapse of Fig. 3. For the velocity exponent we use $\theta \simeq 0.64$ for $\nu_x = 0.4$. However, we find somewhat smaller values of θ as ν_x approaches $\Delta = 3.0$ ($\theta \simeq 0.40$ for $\nu_x = 2.8$). A possible source for this deviation is finite size effects.

[19] K. Sneppen, Phys. Rev. Lett. **69**, 3539 (1992).

[20] H. Leschhorn and L.-H. Tang, Phys. Rev. E **49**, 1238 (1994).

[21] C. Tang, S. Feng, and L. Golubovic, Phys. Rev. Lett. **72**, 1264 (1994).

[22] A. Maritan, F. Toigo, J. Koplik, and J. R. Banavar, Phys. Rev. Lett. **69**, 3193 (1992).

[23] R. Brower, D. Kessler, J. Koplik, and H. Levine, Phys. Rev. A **29**, 1335 (1984); F. David, in *Statistical Mechanics of Membranes and Surfaces*, edited by D. Nelson, T. Piran, and S. Weinberg (World Scientific, Singapore, 1988).

[24] J. Zhang, Y.-C. Zhang, P. Alstrøm, and M. T. Levinsen, Physica A **189**, 383 (1992).

[25] For the QEW universality class, a value $\alpha \simeq 1$ is found when one calculates the roughness exponent using the local width $w(\ell)$ of the interface as a function of the window of observation ℓ [8]. However, due to finite size effects, one usually needs a larger system size than the one considered in this study to obtain this value, which might explain the smaller value obtained in our simulations. The value $\alpha > 1$ can only be obtained by studying the scaling of the total width $W(L)$ with the system size L [10,11].

[26] C. S. Nolle, B. Koiller, N. Martys, and M. O. Robbins, Phys. Rev. Lett. **71**, 2074 (1993)

[27] M. Cieplak and M. O. Robbins, Phys. Rev. B **41**, 11 508 (1990).